Sudden termination of Martian dynamo?: Implications from subcritical dynamo simulations

W. Kuang,[1] W. Jiang,[2] and T. Wang[3]

[1] The crustal magnetism measured by the Mars Global Surveyor requires that Mars possessed a strong internal field generated by a core dynamo in its early history. We use a numerical model to simulate the early Martian dynamo, focusing on the minimum energy for sustaining an established dynamo. Our results show that near its end, the Martian dynamo could reverse frequently, and could be subcritical: the energy to sustain the dynamo is significantly less than that to excite the dynamo. In addition to a longer lifetime, the subcritical dynamo implies that it could be terminated suddenly with a very small perturbation and, once turned off, it could not be reactivated without substantial increase of the buoyancy force in the Martian core. **Citation:** Kuang, W., W. Jiang, and T. Wang (2008), Sudden termination of Martian dynamo?: Implications from subcritical dynamo simulations, *Geophys. Res. Lett.*, *35*, L14204, doi:10.1029/2008GL034183.

1. Introduction

[2] One of the most important findings of the Mars Global Surveyor mission is the strong crustal field in the Martian southern highland [*Acuña et al.*, 1999; *Connerney et al.*, 2001]. Modeling of the global Martian crustal field [*Whaler and Purucker*, 2005; *Mitchell et al.*, 2007] shows that at similar altitudes, the field is much stronger than that of the Earth, suggesting the magnetization acquired in an internally generated magnetic field (via dynamo action) at least comparable in strength to the geomagnetic field [*Schubert et al.*, 2000; *Stevenson*, 2001].

[3] However, debate on the timing of the Martian dynamo is still on-going: how long did it last and when did it stop? Several scenarios have been proposed based on different energy source models, e.g. inner core solidification [*Schubert et al.*, 2000], transitions in the mantle convection processes [*Stevenson*, 2001], or thermodynamic evolution with various geochemical properties [*Williams and Nimmo*, 2004]. Progress has also been made on the timing of the Martian dynamo via correlating the crustal magnetic anomalies with the ages of the craters on the Martian surface [*Arkani-Hamed*, 2004; *Lillis et al.*, 2008a].

[4] To provide a coherent picture, one must address a fundamental question: how much energy is required to sustain an active dynamo and to excite a dynamo? This deserves special attention since, based on the findings that the Martian core field strength was comparable to that of the Earth, similar to the geodynamo, the Martian dynamo could be a strong-field dynamo, i.e. the Lorentz force (from the magnetic field) is comparable to the Coriolis force (from the rotation) and the buoyancy force in much of the Martian fluid core [*Kuang and Bloxham*, 1999; *Kono and Roberts*, 2002].

[5] A strong-field Martian dynamo complicates the energy budget: the minimum energy to sustain an active dynamo can be less than that to excite the dynamo, since the strong Lorentz force reduces significantly the constraints by the Coriolis force on the convection, resulting in smaller buoyancy forces sufficient to drive the dynamo.

[6] *Childress and Soward* [1972] first demonstrated analytically that, once strong-field dynamo action is present, it may continue in a subcritical domain, though the full solutions were not given in their studies. Subcritical strong-field dynamo solutions were later obtained in a numerical simulation of planar layer dynamos [*St. Pierre*, 1993]. Though there are several studies on the energy required for the geodynamo [*Christensen and Tilgner*, 2004], no effort has been focused on subcritical planetary dynamos.

[7] Could the Martian dynamo be subcritical in its final stages? What are the properties of the subcritical Martian dynamo and their broader geophysical implications? Answers to these questions would help us understand the dynamical processes in the Martian core and the evolution of the planet, interpret the observed Martian crustal field, and provide theoretical grounds for future observations. Our approach to address these questions is using a numerical dynamo model to simulate the dynamics associated with the onset and the annihilation of the Martian dynamo.

2. Numerical Model

[8] The numerical model for this study has been developed for the terrestrial dynamos in the past decade [*Kuang and Bloxham*, 1999; *Kuang and Chao*, 2003; W. Jiang and W. Kuang, An MPI-based MoSST core dynamics model, submitted to Physics of the Earth and Planetary Interiors, 2008]. In this investigation, the Martian interior is approximated as follows: the mean radii r_s, r_{cmb}, r_{icb} of the surface, the core-mantle boundary (CMB), and the inner core boundary (ICB) are

$$r_s = 3500 \text{ km}, \quad r_{cmb} = 1600 \text{ km}, \quad r_{icb} = 500 \text{ km}. \quad (1)$$

Above the CMB is a 10 km thick, electrically conducting layer with the magnetic diffusivity $\eta_d = 10\eta$ (η is the magnetic diffusivity of the core fluid).

[1]Planetary Geodynamics Laboratory, NASA Goddard Space Flight Center, Greenbelt, Maryland, USA.
[2]Joint Center for Earth Systems Technology, University of Maryland, Baltimore County, Maryland, USA.
[3]School of Earth Science, Graduate University, Chinese Academy of Science, Beijing, China.

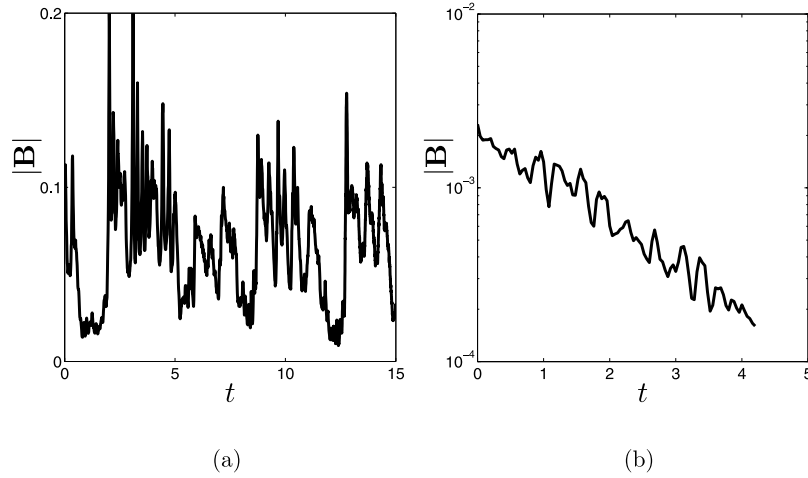(a)   (b)

Figure 1.   The time variation of $|\mathbf{B}|$ for (a) $R_{th} = 2480$ when there is a dynamo solution, and for (b) $R_{th} = 2400$ when there is no dynamo solution. The simulation time t (x-axis) is scaled by the magnetic free decay time $\tau_d (\approx \tau_\eta/\pi^2)$ of the Martian core.

[9] In this model, the partial differential equations describing the core dynamics are non-dimensionalized with r_{cmb} (length scale) and the magnetic diffusive time $\tau_\eta \equiv r_{cmb}^2/\eta$ (time scale). For example, the momentum balance in the core is

$$R_o \frac{D\mathbf{V}}{Dt} + \mathbf{1}_z \times \mathbf{V} = -\nabla p + \mathbf{J} \times \mathbf{B} + R_{th}\Theta\mathbf{r} + E\nabla^2\mathbf{V}, \quad (2)$$

where $\mathbf{V}$ is the fluid velocity, $\mathbf{B}$ is the magnetic field, $\mathbf{J} \equiv \nabla \times \mathbf{B}$ is the current density, Θ is the fluid density perturbation, p is the modified pressure, $\mathbf{r}$ is the position vector and $\mathbf{1}_z$ is the normal vector of the rotation axis. The Rayleigh number R_{th} in (2) describes the buoyancy force that can be thermal, or compositional, or both. The rapid rotation of Mars results in very small magnetic Rossby number R_o and Ekman number E:

$$R_o \approx 10^{-8}, \quad E \approx 10^{-14}. \quad (3)$$

Due to computational constraints, they are much larger in numerical simulations, e.g. in this study,

$$R_o = E = 1.25 \times 10^{-6}. \quad (4)$$

The impact of the parameter difference will be discussed later. The state variables ($\mathbf{V}$, $\mathbf{B}$, Θ) are approximated with spherical harmonic expansions up to degree L and order M. The spectral coefficients in the expansions are discretized on the radial grid points $\{r_i | i = 0,1,\ldots,N\}$. In the simulations reported here, $L \times M \times N = 76^3$.

[10] The minimum energies for the dynamo onset and termination are given by the two critical Rayleigh numbers R_{cf} and R_{cr}, respectively. To obtain the first critical point R_{cf}, the simulation starts from a small R_{th} at which there is no dynamo solution. Then R_{th} increases gradually until a stable dynamo solution is found. This is hereafter called the forward simulation process. To locate R_{cr}, the simulation process is reversed (and hereafter referred to as the reverse simulation process): the simulation starts with a large R_{th} at

which a well developed strong-field dynamo solution exists. Then R_{th} decreases gradually until no dynamo solution is found in the simulation. For each R_{th}, the simulation starts from an initial state and ends when a well developed solution is obtained. To closely track the variation of the dynamo with R_{th}, the initial condition is chosen from the numerical solutions of the preceding Rayleigh number. In this study, the reverse process is carried out first since there are many simulated strong-field dynamo solutions [*Kuang and Bloxham*, 1999; *Kuang and Chao*, 2003].

[11] The existence of dynamo action can be judged by the time variation of the mean magnetic field strength

$$|\mathbf{B}| \equiv \left[\frac{1}{V_{oc}} \int_{V_{oc}} |\mathbf{B}|^2 dv\right]^{1/2} \quad (5)$$

over the core volume V_{oc}. For example, Figure 1 shows the time variations of $|\mathbf{B}|$ for $R_{th} = 2480$ (Figure 1a) and $R_{th} = 2400$ (Figure 1b). In the former there is a dynamo solution, and $|\mathbf{B}|$ remains finite through out the simulation time. In the latter, the convection can not sustain a dynamo action, and $|\mathbf{B}|$ decays exponentially in time. With the definition (5),

$$|\mathbf{1}_z \times \mathbf{V}| \approx |\mathbf{J} \times \mathbf{B}| \approx R_{th}|\Theta\mathbf{r}| \quad (6)$$

in the strong-field dynamos.

3.   Results

[12] The overall numerical results are summarized in Figure 2. The magnetic field strength in the figure is the time-averaged field strength

$$\overline{|\mathbf{B}|} \equiv \frac{1}{T} \int_0^T |\mathbf{B}| \, dt \quad (7)$$

over the simulation period T for a given R_{th}. Figure 2a shows the $\overline{|\mathbf{B}|}$ for both the reverse (solid line) and the forward (dashed line) processes. When the Rayleigh number decreases from $R_{th} = 15000$ to $R_{th} = 2460$, $\overline{|\mathbf{B}|}$ remains the
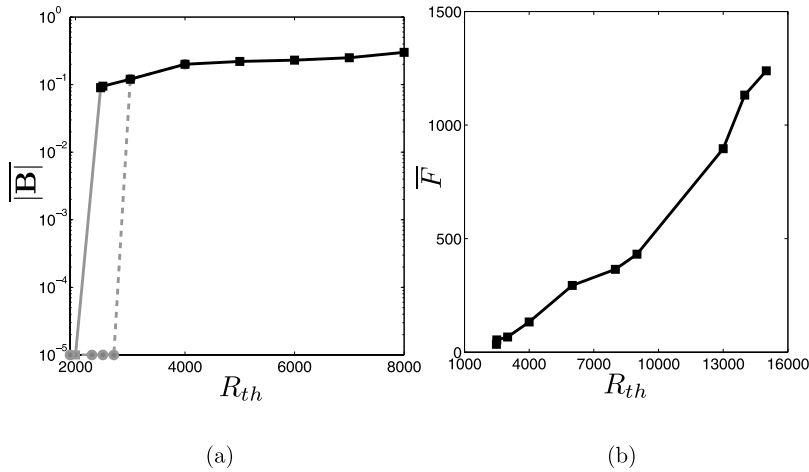
(a)   (b)

Figure 2. The variation of (a) the time-averaged $\overline{|\mathbf{B}|}$ and (b) the time-averaged $\overline{F}$ for different Rayleigh numbers R_{th}. The solid lines are for the reverse simulation process, and the dashed line is for the forward simulation process. The grey segments correspond to non-dynamo states.

same order of magnitude. However, as R_{th} decreases from 2460 to 2420 (less than 2% reduction), $\overline{|\mathbf{B}|}$ drops by more than an order of magnitude. At R_{th} = 2420, $|\mathbf{B}|$ decays very slowly in time. No dynamo is found at R_{th} = 2400 (Figure 1b). Therefore the estimated critical point for the termination of the dynamo is $R_{cr} \approx 2440$. More accurate estimation needs substantially longer simulation time, because the closer to the critical point, the slower the exponential decay of $|\mathbf{B}|$.

[13] The forward process starts from R_{th} = 1900. No dynamo solution is found until R_{th} = 3000. Between the two numbers, the core is in pure convection. Above R_{th} = 3000, dynamo solutions are found with the field strength $|\mathbf{B}|$ similar to those in the reverse process. Thus the estimated critical point for the onset of dynamo is $R_{cf} \approx 3000$, approximately 25% greater than R_{cr}. Therefore, the dynamo solutions (from the reverse process) in the domain $R_{cr} < R_{th} < R_{cf}$ are subcritical.

[14] Are the subcritical dynamos the strong-field dynamos, as argued in the past studies [*Childress and Soward*, 1972; *St. Pierre*, 1993]? To examine this, we consider whether the second part of (6), i.e.

$$F \equiv |\mathbf{J}||\mathbf{B}|/|\Theta| \propto R_{th} \qquad (8)$$

holds for the dynamo solutions. In Figure 2b are the time-averaged $\overline{F}$ for different R_{th}. Clearly $\overline{F}$ increases approximately linearly with R_{th}, thus agreeing well with (8).

[15] The morphologies of the magnetic field at the CMB and therefore at the surface are very different between the supercritical and subcritical domains. In the supercritical domain ($R_{th} \geq R_{cf}$), the magnetic field is dominantly axially dipolar. However, this dominance is weakened in the subcritical domain ($R_{cr} \leq R_{th} \leq R_{cf}$). Since the radial component B_r of the magnetic field is described by a spherical harmonic expansion with the spectral coefficients $\{b_{lm}\}$ of degrees l ($l \geq 1$) and orders m ($m \leq l$), the absolute angle of the dipole axis to the rotation axis is $\xi \equiv \sin^{-1}[|b_{11}|/(|b_{10}|^2 + |b_{11}|^2)^{1/2}]$. For example, for R_{th} = 4000 (supercritical), the mean $\overline{\xi} \approx 1°$; for R_{th} = 2480 (subcritical), $\overline{\xi} \approx 49°$.

[16] This large tilt of the magnetic pole to the rotation axis at R_{th} = 2480 arises from the frequent magnetic polarity reversals: there are 4 reversals, and 6 excursions over 30 magnetic free-decay time, i.e. approximately one reversal per 8 magnetic free-decay time. In Figure 3 are the snapshots of the B_r at the surface during a complete reversal process.

4. Geophysical Implications

[17] If qualitatively applicable to Mars, these numerical results may have several significant geophysical implications on the early Martian magnetic and dynamic history.

[18] A subcritical Martian dynamo has several consequences. First, it should have terminated over a very short period. For example, assuming that the Rayleigh number R_{th} decreases linearly in time, and that the dynamo lasted approximately 500 Ma, then the termination could have occurred in less than 5 Ma (i.e. 1% of 500 Ma), since a less than 1% reduction in R_{th} near R_{cr} is sufficient to shut down the dynamo action.

[19] Because the magnetic field intensity of the subcritical dynamos remains comparable to those of the supercritical strong-field dynamos (Figure 2a), the Martian crustal magnetization could have occurred in a strong core field during the entire acquisition history. Once a subcritical Martian dynamo is turned off by a small perturbation (<1%) to the buoyancy force (R_{th}), it could not be reactivated when the perturbation disappears. The reactivation is only possible with a substantial increase of the driving force, since the supercritical point R_{cf} for the onset of dynamo is nearly 25% higher than R_{cr}. To a thermally driven Martian dynamo, for example, the heat flow across the CMB is proportional to the Rayleigh number R_{th}. This implies that near the subcritical point R_{cr}, a less than 1% perturbation to the heat flow is sufficient to turn off the dynamo; while a 25% increase is necessary for the reactivation.

[20] The lifetime of the Martian dynamo could increase significantly because of the subcritical dynamo. This increase is proportional to the difference $R_{cf} - R_{cr}$ (the
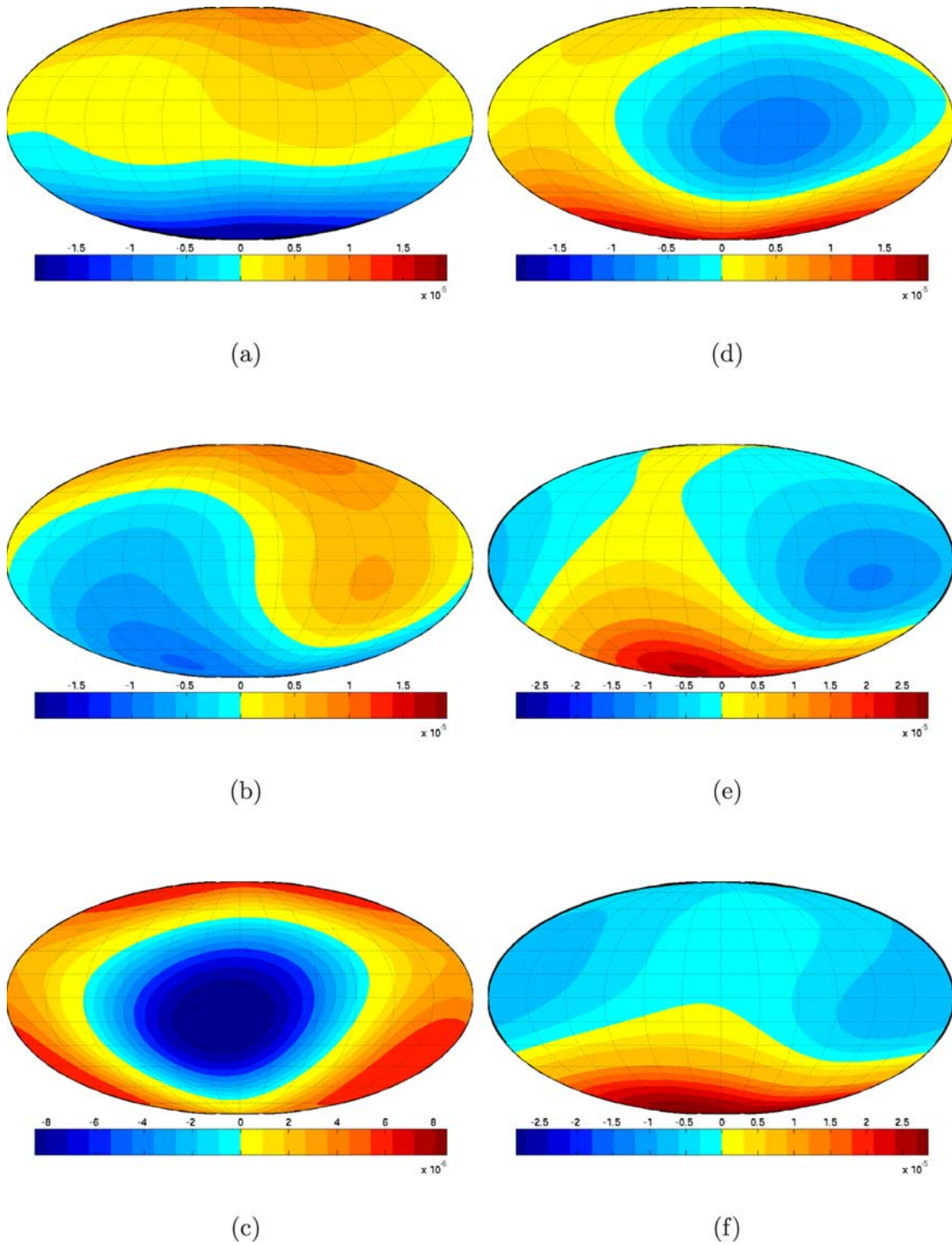
Figure 3. A series of snapshots of B_r at the surface of Mars from (a) the beginning to (f) the ending of a polarity reversal at $R_{th} = 2480$. The blue means $B_r < 0$ (inward) and orange means $B_r > 0$ (outward).

subcritical domain). Again if R_{th} decays linearly in time, the increase could be as much as 25% of the expected life defined by R_{cf}, e.g. 125 Ma for a 500 Ma estimated life. This certainly adds a new dimension in the conjectures on the timing of the Martian dynamo and the planet's early thermal evolution history [*Schubert et al.*, 2000; *Stevenson*, 2001].

[21] The magnetic field morphologies of the subcritical dynamos are very different from those of the supercritical dynamos. This difference may also have consequences on the Martian crustal magnetization. Numerical results show that the poloidal magnetic field of the subcritical dynamos is not axially dipolar, e.g. with the mean 49° angle between the actual dipole and the rotation axis at the Rayleigh numbers slightly above the subcritical point R_{cr}. Provided that these morphologies lasted over a long period to impact the crustal magnetization, this mid-latitude magnetic dipole

should be included in the studies of inferring polar wander based on magnetic anomalies [*Arkani-Hamed and Boutin*, 2004; *Hood et al.*, 2005; *Langlais and Purucker*, 2007].

[22] Our results are consistent with several recent studies on the Martian crustal magnetism and on the dating of craters at the Martian surface [*Lillis et al.*, 2008b; *Frey*, 2008]. These studies suggest that the Martian dynamo was terminated in a very short period ($<10^7$ years) in the period when a series of giant impacts hit the Martian surface. Numerical modeling suggests that the impacts could perturb the heat flow across the CMB by several percents in magnitude [*Roberts et al.*, 2008].

[23] If measurements on the Martian magnetic paleo-intensity and the paleo-polarity could be made, and such measurements could show strong paleo-intensities, and reversals in the later Martian dynamo period, then they would provide further support for the existence of subcritical Martian dynamos.

[24] It should be pointed out that the numerical simulations do have limitations. Among them are the difference between the parameters (3) estimated for Mars, and those (4) used in the simulations, and a finite inner core in the numerical model. The parameter differences may certainly affect the numerical solutions, including the critical points R_{cf} and R_{cr}. They also limit the quantitative interpretations of the geophysical quantities (e.g. magnetic field intensity and heat flow across the CMB). However, they should not change qualitatively the dynamics since, as shown in Figure 2b, the leading order force balance is established among the Coriolis force, the Lorentz force and the buoyancy force. The fluid inertia (with R_o) and the viscous force (with E) are of higher order significance.

[25] Existence of a finite inner core in the model deserves special attention: what are the impacts of the inner core on the subcritical Martian dynamos? For example, earlier studies in numerical dynamo simulations suggest that the inner core plays an important role in the magnetic polarity reversals [*Hollabach and Jones*, 1993]. Our numerical solutions show also frequent reversals near the subcritical point R_{cr}. Could this be the consequence of the inner core used in our model? The knowledge about the Martian core is still very limited, and several scenarios are discussed in relation to the Martian dynamo and core formation [*Stevenson*, 2001]. Obviously our current model with a finite inner core fits well to the scenario that the Martian dynamo started with the solidification of an inner core [*Schubert et al.*, 2000]. Other scenarios could also be possible, such as fast cooling of the core due to efficient mantle convection [*Nimmo and Stevenson*, 2000; *Williams and Nimmo*, 2004]. In this case, solidification of the inner core may not necessarily occur during the dynamo era. Recent high-pressure experiment, however, suggests that Martian inner core formation is very different from that of the Earth [*Stewart et al.*, 2007]. Further numerical simulations could help differentiate these scenarios.

References

Acuña, M. H., et al. (1999), Global distribution of crustal magnetization discovered by the Mars Global Surveyor MAG/ER experiment, *Science*, *284*, 790–793.

Arkani-Hamed, J. (2004), Timing of the Martian core dynamo, *J. Geophys. Res.*, *109*, E03006, doi:10.1029/2003JE002195.

Arkani-Hamed, J., and D. Boutin (2004), Paleomagnetic poles of Mars: Revisited, *J. Geophys. Res.*, *109*, E03011, doi:10.1029/2003JE002229.

Childress, S., and A. M. Soward (1972), Convection-driven hydromagnetic dynamo, *Phy. Rev. Lett.*, *29*, 837–839.

Christensen, U. R., and A. Tilgner (2004), Power requirement of the geodynamo from ohmic losses in numerical and laboratory dynamos, *Nature*, *429*, 169–171.

Connerney, J. E. P., M. H. Acuña, P. J. Wasilewski, G. Kletetschka, N. F. Ness, H. Réme, R. P. Lin, and D. Mitchell (2001), The global magnetic field of Mars and implications for crustal evolution, *Geophys. Res. Lett.*, *28*, 4015–4018.

Frey, H. (2008), Ages of very large impact basins on Mars: Implications for the later heavy bombardment in the inner solar system, *Geophys. Res. Lett.*, *35*, L13103, doi:10.1029/2008GL033515.

Hollabach, R., and C. Jones (1993), Influence of the Earth's inner core on geomagnetic fluctuations and reversals, *Nature*, *365*, 541–543.

Hood, L. L., C. N. Young, N. C. Richmond, and K. P. Harrison (2005), Modeling of major Martian magnetic anomalies: Further evidence for polar reorientation during the Noachian, *Icarus*, *177*, 144–173.

Kono, M., and P. H. Roberts (2002), Recent geodynamo simulations and observations of the geomagnetic field, *Rev. Geophys.*, *40*(4), 1013, doi:10.1029/2000RG000102.

Kuang, W., and J. Bloxham (1999), Numerical modeling of magnetohydrodynamic convection in a rapidly rotating spherical shell: weak and strong field dynamo action, *J. Comput. Phys.*, *153*, 51–81.

Kuang, W., and B. F. Chao (2003), Geodynamo modeling and core-mantle interactions, in *Earth's Core: Dynamics, Structure, Rotation, Geodyn. Ser.*, vol. 31, edited by V. Dehant et al., pp. 193–212, AGU, Washington, D. C.

Langlais, B., and M. Purucker (2007), A polar magnetic paleopole associated with Apollinaris Patera, *Planet. Space Sci.*, *55*, 270–279.

Lillis, R. I., H. V. Frey, M. Manga, D. L. Mtichell, R. P. Lin, M. H. Acuña, and S. W. Bougher (2008a), An improved crustal magnetic field map of Mars from electron reflectometry: Highland volcano magmatic history and the end of the Martian dynamo, *Icarus*, *194*, 575–596.

Lillis, R. I., H. Frey, and M. Manga (2008b), Rapid decrease in Martian crustal magnetization in the Noachian era: Implications for the climate and interior of early Mars, *Geophys. Res. Lett.*, doi:10.1029/2008GL034338, in press.

Mitchell, D. L., R. J. Lillis, R. P. Lin, J. E. P. Connerney, and M. H. Acuña (2007), A global map of Mars crustal magnetic field based on electron reflectometry, *J. Geophys. Res.*, *112*, E01002, doi:10.1029/2005JE002564.

Nimmo, F., and D. J. Stevenson (2000), Influence of early plate tectonics on the thermal evolution and magnetic field of Mars, *J. Geophys. Res.*, *105*, 11,969–11,979.

Roberts, J., R. J. Lillis, M. Manga, and H. V. Frey (2008), Impact-related heating and the cessation of the Martian dynamo: Early results, *Proc. Lunar Planet. Sci. Conf. 39th*, 1358.

Schubert, G., C. T. Russell, and W. B. Moore (2000), Timing of the Martian dynamo, *Nature*, *408*, 666–667.

Stevenson, D. J. (2001), Mars' core and magnetism, *Nature*, *412*, 214–219.

Stewart, A. J., M. W. Schmidt, W. van Westrenen, and C. Liebske (2007), Mars: a new core-crystallization regime, *Science*, *316*, 1323–1325.

St. Pierre, M. G. (1993), The strong field branch of the Childress-Soward dynamo, in *Solar and Planetary Dynamos: Proceedings of NATO Advanced Study Institute*, edited by M. R. E. Proctor et al., pp. 295–302, Cambridge Univ. Press, Cambridge, U. K.

Whaler, U. A., and M. E. Purucker (2005), A spatially continuous magnetization model for Mars, *J. Geophys. Res.*, *110*, E09001, doi:10.1029/2004JE002393.

Williams, J. P., and F. Nimmo (2004), Thermal evolution of the Martian core: Implications for an early dynamo, *Geology*, *32*, 97–100.

————————

W. Kuang, Planetary Geodynamics Laboratory, Mail Stop 698, NASA Goddard Space Flight Center, Greenbelt, MD 20771, USA. (weijia.kuang-1@nasa.gov)

W. Jiang, Joint Center for Earth Systems Technology, University of Maryland, Baltimore County, Baltimore, MD 21250, USA. (jiangw@umbc.edu)

T. Wang, School of Earth Science, Graduate University, Chinese Academy of Science, Beijing 10049, China. (tywang@mails.gucas.ac.cn)